Improved Machine Vision for Single Cell Printing

D. Liang[1], A. Gross[1], J. Schöndube[1], S. Rubenwolf[1], A. Yusof[1], A. Ernst[1,2], R. Zengerle[1], G. Roth[1] and P. Koltay[1,2]
[1] Laboratory for MEMS Applications, IMTEK, University of Freiburg, Germany
[2] BioFluidix GmbH, Georges Köhler Allee 106, 79110 Freiburg, Germany
Dong.Liang@imtek.de

Abstract

We present a **machine vision system for single cell printing**. Focus here is on individual living cells, more precisely on certain tissue stem cells and cancer stem cells. These biological cells are optically imaged inside a microfluidic dispenser chip by a monochrome smart camera with digital signal processor (DSP) for **real-time image processing**. Coaxial illumination and parallel image acquisition make **high speed cell detection** possible. In our first experiment with HeLa cells the maximum image processing frequency reached **125 Hz**, which is about **16 times faster than previously achieved** [1]. The yield of successful cell detection reached 89 % in the first experiments.

Kurzfassung

Für die Anwendung im Rahmen des Einzelzell-Dosierens präsentieren wir ein **maschinelles Bildverarbeitungssystem**. Der Fokus liegt dabei auf einzelnen, lebenden Zellen, genauer auf verschiedenen Gewebestammzellen und Krebsstammzellen. Diese biologischen Zellen, welche sich im Inneren eines mikrofluidischen Chips befinden, werden optisch durch eine monochrome Kamera mit integriertem digitalem Signalprozessor (DSP) für **Echtzeit-Bildverarbeitung** beobachtet. Koaxiale Beleuchtung und parallele Bildaufnahme gestatten so eine **Hochgeschwindigkeitsdetektion** der Zellen im Chip. In ersten Experimenten mit HeLa Zellen konnte gezeigt werden, dass die Bildverarbeitungsfrequenz **125 Hz** erreichen kann, was **um einen Faktor 16 schneller ist, als die Ergebnisse vorheriger Arbeiten** [1]. Die Rate korrekter Zellerkennungen lag dabei in ersten Experimenten bei 89 %.

1 Introduction

Single cell printing has nowadays opened up a new dimension in cell biology, tissue engineering, drug development and diagnostics. Compared to cell detection methods with labeling such as fluorescence activated cell sorting (FACS) or dielectrophoresis activated cells sorting (DACS) [2], machine vision offers another attractive alternative for detection of cell types that cannot be labeled. Besides the feasibility and validity of cell detection, recognition speed and real-time processing by machine vision systems are also of great interest for single cell detection in particular for cell printing applications.

In former work [1] the feasibility of single cell printing with a machine vision system has been demonstrated. A non-contact dispenser chip based on the NanoJet technology [3] generates free flying picoliter droplets which contain the cells. The NanoJet has a transparent glass surface, thus the cell flow can be observed visually. During dispensing a camera captures images near the dispenser nozzle. If no cell or several cells are detected in the vicinity of the nozzle, which is judged by the machine vision system, the cells will be expelled towards a waste position with the subsequent dispense. If the machine vision system finds only one single cell close to the nozzle, the following droplet will be directed towards the desired target position to print the single cell.

After proof of principle the machine vision has been improved like reported in the following. The machine vision now delivers images with better quality, 16 times faster processing frequency and real-time cell detection in comparison to our old work. With these benefits the new single cell printing system it is expected to greatly increase throughput and dispensing yield for single cell printing applications.

2 Description of systems

2.1 Hardware and print head

The presented machine vision system consists of a smart CCD camera, a coaxial illumination LED and a zoom optic. It is mounted together with the dispenser (customized P9 dispenser, BioFluidix GmbH, Germany) to form the so called print head of the single cell printing machine (Figure 1). Details of the dispensing method as well as machine concept and approach can be found in [5, 6].

The machine vision system employs a smart camera with onboard digital signal processor (DSP) and monochrome CCD sensor (Vision Components VC4458). All tasks of image processing are only accomplished by the DSP. In contrast to our previous work whereas all imaging processing was proceeding in the PC, the smart camera supports real-time image acquisition and processing. All computing tasks in the DSP are transparent to the programmer and the scheduling is more exactly predictable. Through trigger ports and digital I/O's the smart camera can communicate with the dispenser and axes stage in real-time. As color information is not critical in our application, we refrained from using a color sensor and selected a

ISBN 978-3-8007-3367-5

monochrome sensor to gain better light sensitivity and acquisition speed.

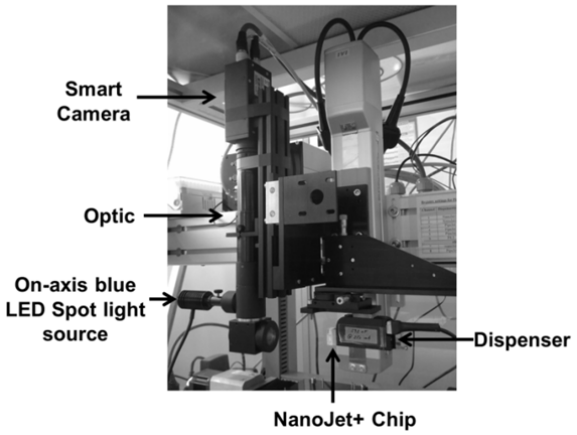

Figure 1 Print head consisting of machine vision system (camera, optics, LED) and non-contact dispenser

The optical components used in our machine vision system integrates two fixed magnification object lenses, one zoom objective, one coaxial light source mount and one 90° deflection mirror (Stemmer Imaging GmbH, custom product). Totally it generates a variable magnification from 1.4x to 10.2x and a depth of field of about 55µm. Together with 1/3" sensor of our smart camera this machine vision system could take a field of view from 471x353 µm² up to 3429x2571 µm². At the largest magnification one cell with diameter of 10µm contains about 185 pixels.

A coaxial 470 nm LED spot light source (max. power consumption 3 W) realizes bright field illumination. Compared to our previous work with dark field illumination, our new machine vision system with bright field illumination supports much shorter shutter time. Shorter shutter time contributes to increase of image acquisition frequency.

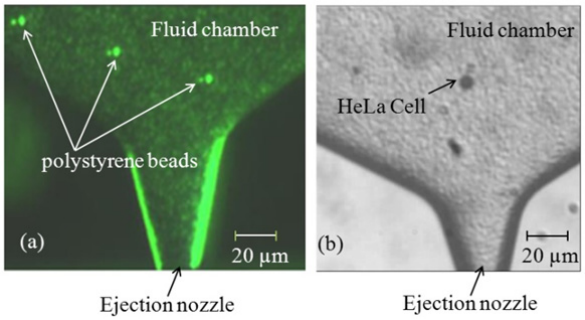

Figure 2 (a) Dark field image from previous work showing polystyrene beads in the dispenser chip [1] (b) Bright field image from new machine vision system showing a HeLa cell.

2.2 Parallel image acquisition and processing procedure

One cell detection cycle in the machine vision system consists of three steps: **Exposure** (expose, readout sensor), **Transfer** (digitize image, save to RAM) and **Processing** (image processing algorithms, result generation). In order to shorten cycle times these three steps are performed in parallel (Figure 3), which can save theoretically up to 66.7 % in time compared to serial processing.

1. Image	Exposure 1	Transfer 1	Processing 1		
2. Image		Exposure 2	Transfer 2	Processing 2	
3. Image			Exposure 3	Transfer 3	Processing 3
4. Image				Exposure 4	Transfer 4
5. Image					Exposure 5

Figure 3 Schematic of parallel image acquisition [7]

A benchmark of serial and parallel image acquisition and processing procedure is shown in Table 1. In case of standalone image acquisition (no processing) the total cycle time in serial operation is 6.2 ms while in parallel mode it is 4.2 ms. These values illustrate the hardware limitation of the presented machine vision system. Our image processing algorithm for cell recognition usually takes about 8 ms for processing an image of 296x296 pixels². About 6.2 ms cycle time could be saved by the operation in parallel mode.

	standalone image acquisition (no processing)	**image acquisition with processing**
Exposure Time [ms]	2	2
Transfer Time [ms]	4.2	4.2
Processing Time [ms]	0	8
Cycle Time (serial) [ms]	6.2	14.2
Cycle Time (parallel) [ms]	4.2	8

Table 1 Cycle time of serial and parallel image acquisition and processing for images of 296x296 pixels

The image processing program detects whether the next droplet to be created will contain one single cell, more than one cell or no cell. To achieve this, the captured image (Figure 4(a)) is compared pixel by pixel with a reference image that contains no cell. In the resulting difference image (Figure 4(b)) the cells appear as bright gray blobs in front of darker background. A following binarization step isolates the cells from background (Figure 4 (c)). The center of gravity of detected cells is shown in the positioning image (Figure 4 (d)).

The binarization threshold can be selected manually or by implemented auto threshold algorithms. In our machine vision system we implemented 16 different pixel based auto threshold algorithms known from literature (Figure 5) [8]. With help of these auto thresholds the user can find easily a suitable threshold for cells with different optical properties.

 ISBN 978-3-8007-3367-5

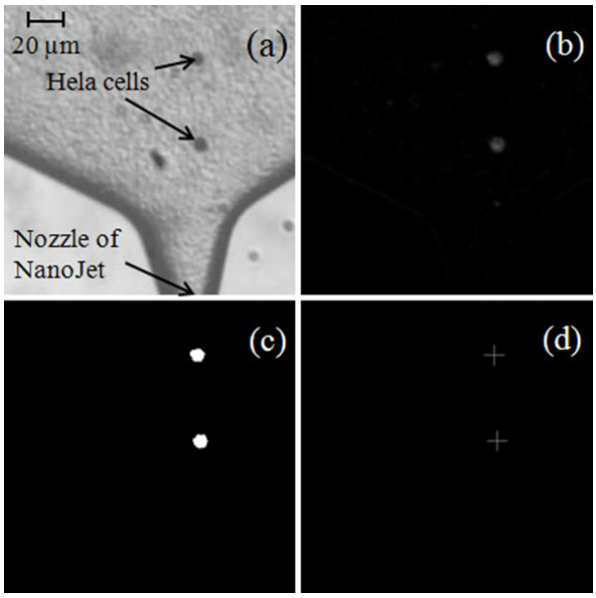

Figure 4 (a) original captured image with HeLa cells inside dispenser (b) difference image (c) binary image with detected cells (d) positions of detected cells

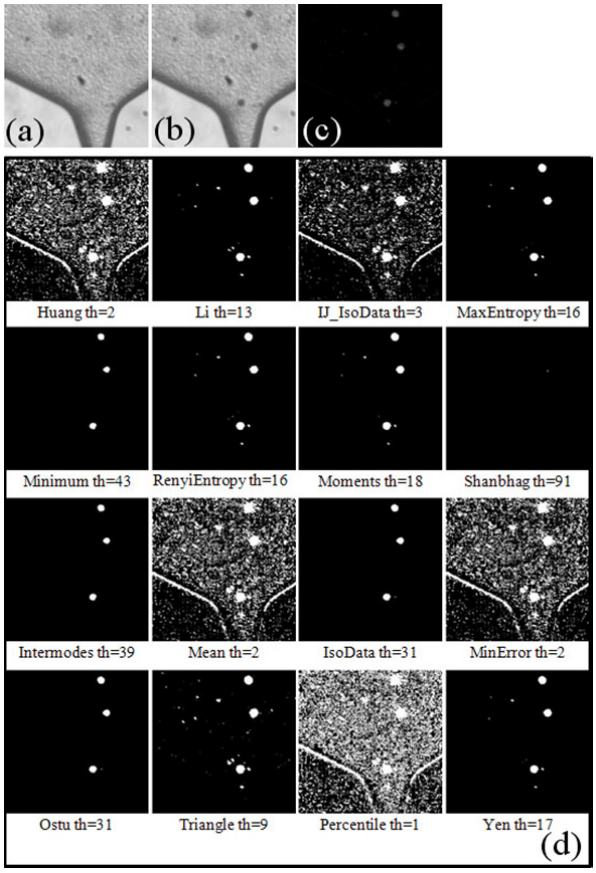

Figure 5 (a) reference image without cells inside dispenser (b) example image with HeLa cells (c) difference image (d) results of auto threshold algorithms [8]

Ultimately the quantity, size in pixels and position of recognized cells are exported to an accessible data file (at additional costs for the cycle time). However, besides cells movable dust, overlapped cells (cell aggregates) and any geometries appearing due to vibrations are also detected by the processing program. Selecting a suitable threshold, as well as size filtering help to reduce these so called detection faults.

3 Experiment and results

We designed the following experiment to study the performance of our new machine vision system. While dispensing HeLa cells (about 10 µm diameter) the image processing system captured 100 images of 296x296 pixels. We stored the capture images and compared the machine vision processing results with what we observed by eye on the images.

10.2x magnification and maximum illumination (about 700 mA operating current) was used in this experiment. The boundaries of size filter were empirically set up to be 100 and 300 pixels. A threshold value of 35 was manually chosen to best fit the conditions. The cycle time was 8 ms.

Examples of detection faults are shown in Figure 6 and their occurrence in this experiment is quantified in Table 2. All faults were successfully filtered out. However, in 17 images moveable dust were detected and filtered out, even in those images the dust was not visible for the operator. In two of these images cells were obviously incorrectly filtered out as moveable dust. And in two images one large cell was detected as overlap and filtered out.

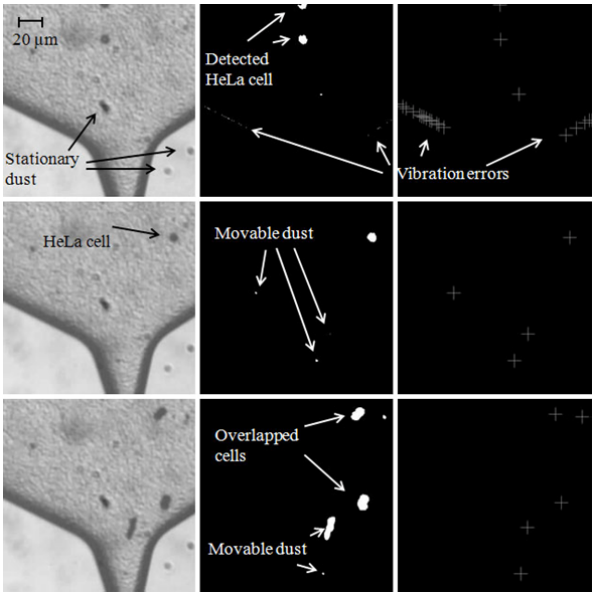

Figure 6 Detection faults due to stationary dust, vibrations, movable dust and cell overlaps

fault type	visually observed	automatically detected and filtered	filter algorithms
stationary dust	100%	100%	difference with reference
vibration	3%	3%	size criterion
moveable dust	65%	82%	size criterion
overlapped cells	5%	7%	size criterion

Table 2 Occurrence of fault types

Because this detection algorithm is based on gray scale difference, the cells with bad contrast to the background are hardly to be correctly detected. In this experiment we observed several cells that merged in the shadow of channel borders or stationary dust (Figure 7, Table 3). Some cells were detected as rings due to reflection or transparence in the center (Figure 7, Table 3).

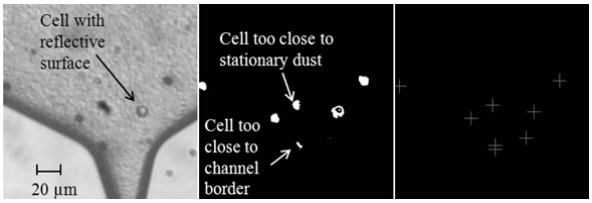

Figure 7 Hardly or incorrectly detected cells

incorrectly detected cell types	visually obersverd	automatically detected
Cells overlapped with stationary dust	1%	0%
Cells merged in boundary	7%	0%
Cells detected as rings	13%	10%

Table 3 Occurrence of incorrectly detected cells

In 89 captured images of this experiment the cells were correctly detected. 39 images were detected to have single cells and 37 of them were correct compared to human observation. Therefore successful detection rate in this experiment reached 89 % while in the case of single cells the successful detection rate reaches 95 %. In contrast to our previous work, the most significant improvement is the detection frequency, which is about 16 times faster than previously (Table 4).

	successful detection rate	max. detection freq.	frame rate of camera	min. shutter time
Previous Work	92%	8Hz	30fps	24ms
Present Work	89% (95% for single cell)	125Hz	242fps	2ms

Table 4 Benchmark of previous and present machine vision system for single cell dispensing

4 Conclusion and outlook

In this article we have presented the optical hardware, image recognition software and first experimental results of a high-speed real-time machine vision system for single cell dispensing. The performance of this improved machine vision system has been quantified by first experiments using HeLa cells. With image size of 296x296 pixels^2 the overall min. cycle time for complete cell detection reaches 8 ms which is about 16 times faster than previous work. Successful detection rate of cells reaches overall 89% and 95% for single cells. The detection rate is compromised by faults due to stationary dust, vibration (occurrence rate 3%), movable dust (occurrence rate more than 65%) and cell overlaps (occurrence rate 5%).

In subsequent experiment the machine vision system will be operated in our single cell printing system for further experiments with different cell types. Constant improvement of detection algorithms and optical hardware will also be part of future work.

5 Acknowledgements

This work was funded by the BMBF (Project ZEPTO, FKZ 16SV50066) and the European Comission (Project PASCA, www.pasca.eu, GA Number: 257073).

6 Literature

[1] A. Yusof, H. Keegan, C.D. Spillane, O.M. Sheils, C.M. Martin, J.J. O`Leary, R. Zengerle, and P. Koltay, “Inkjet-like printing of single-cells,” Lab on a chip, Jun. 2011, pp. 6-10..

[2] H. M. Davey and D.B. Kell. Flowcytometry and cell sorting of heterogeneous microbial populations: The importance of single- cell analyses. Microbiol. Rev. 60:641–661, 1996.

[3] P. Koltay, R. Steger, G. Birkle, H.-C. Huang, H. Sandmaier, R. Zengerle. Microdispenser array for highly parallel and accurate liquid handling. SPIE’s International Symposium on Microelectronics and Micro-Electro-Mechanical Systems. 17.-19. 2001

[4] J. Schöndube, A. Yusof, A. Gross, S. Rubenwolf, D. Liang, G. Roth, R. Zengerle and P. Koltay. Automatisiertes Drucken einzelner Zellen mittels eines kontaktfreien Druckverfahrens im Picoliterbereich, Mikrosystemtechnik Kongress 2011.

[5] S. Rubenwolf, S. Niekrawietz, J. Schöndube, A. Gross, A. Yusof, D. Liang, P. Koltay, R. Zengerle and G. Roth. Digitaler Druck einer Hydrogelmatrix für das Einbetten von Zellen in künstlichen Zellverbänden. Mikrosystemtechnik Kongress 2011.

[7] Vision Components. Programming tutorial basics for VC Smart cameras with Ti DSP. 2008.

[8] G. Landin. Auto threshold, http://pacific.mpi-cbg.de/wiki/index.php/Auto_Threshold, accessed 2011.

 ISBN 978-3-8007-3367-5